ELSEVIER

S0032-3861(96)00413-2

Polymer Vol. 37 No. 25, pp. 5589–5596, 1996

0032-3861/96/$15.00 + 0.00

Binary blends of a new wholly aromatic thermoplastic polyimide and poly(ether imide)

Shi Ping Ma and Toshisada Takahashi*
Faculty of Engineering, Fukui University, Bunkyo 3-9-1, Fukui 910, Japan
(Received 30 October 1995; revised 16 February 1996)

This present investigation deals with the miscibility, phase behaviour and semicrystalline morphology of new thermoplastic polyimide (N-TPI)/poly(ether imide) (PEI) blends with different compositions. Melt-quenched amorphous blends were used as the raw materials. The phase behaviour of the blends has been studied by means of differential scanning calorimetry (d.s.c.). It has been found that the following four states develop depending upon the heat-treatment temperature and the blend composition: (1) a miscible amorphous state in the melt-quenched blends, (2) a phase-separated amorphous state in the blend that had been heat treated at 260°C, (3) a semicrystalline state with phase-separated amorphous regions in the blends that had been heat treated at 290–340°C, and (4) a semicrystalline state with miscible amorphous regions in the blends that had been heat treated at temperatures above 350°C. The semicrystalline morphology of the blends corresponding to the above four states was studied by means of small-angle X-ray scattering (SAXS). The results were analysed on the basis of the one-dimensional correlation function proposed by Stroble and coworkers. It has been found that the long-period and the amorphous thickness of the blends increase with increasing PEI content. The d.s.c. and SAXS studies of the blends lead to the conclusion that the PEI segments are incorporated in the amorphous layer between the stacked N-TPI crystals, regardless of the phase separation. Copyright © 1996 Elsevier Science Ltd.

(Keywords: polyimide; poly(ether imide); binary blends)

INTRODUCTION

During the last decade, various kinds of wholly aromatic thermoplastic polymers such as poly(arylether ketone)s (PAEKs), polysulfones, poly(ether nitrile)s, poly(ether sulfone)s, and polyimide have been developed. These polymer materials have excellent mechanical properties, high operating temperatures, and high solvent resistances. Blends of these aromatic polymers can be expected to find increasing practical applications in the field of polymer engineering. Miscible blends of poly(ether ether ketone) (PEEK) and the poly(ether imide) [PEI: poly(2,2′-bis(3,4-dicarboxyphenoxy) phenyl propane)-2-phenylene bis imide] have been studied by several workers, and the miscibility, semicrystalline morphology, crystallization kinetics and melting behaviour have been examined[1–7]. Mutual blends of various PAEKs and blends of modified PAEKs with aromatic polyimides were also studied by Harris and Robeson[8], and Porter[9].

Recently a new wholly aromatic thermoplastic polyimide (N-TPI) was synthesized from 4,4′-bis(3,3′-aminophenoxy)biphenyl and pyromellitic dianhydride; its chemical formula is as follows:

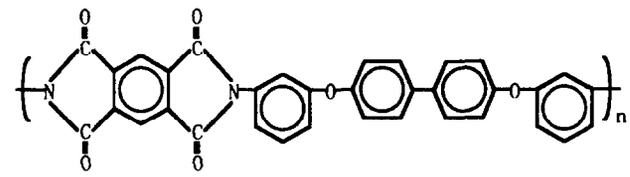

N-TPI is a semicrystalline polymer with a glass transition temperature (T_g) of 250°C and a melting temperature (T_m) of 380°C; the material exhibits a high T_g/T_m ratio of 0.79. (The T_g/T_m ratios of PAEKs are usually in the range from 0.64 to 0.69.) N-TPI has, therefore, attracted the attention of many workers. In particular, the crystal structure[10], semicrystalline morphology[11,12], thermal and crystallization behaviour[13,14], and the development of its supermolecular structure during drawing and rolling[15,16] have been reported by various workers.

Blends of N-TPI with various PAEKs have been studied by several workers[17–19]. Furakawa *et al.* found that the crystallization rate of N-TPI in the blends was accelerated in the presence of the PAEKs[17]. It has also been shown that the processability of N-TPI can be modified by the addition of poly(ether ketone) (PEK)[18]. Sauer and Hsiao examined the miscibility of N-TPI with

* To whom correspondence should be addressed

three different PAEKs. It has been reported that N-TPI is miscible with PEEK and PEK to some extent, but N-TPI, however, is immiscible with poly(ether ketone ketone) (PEKK)[19].

In this present investigation, the miscibility, phase behaviour, crystallization behaviour, and supermolecular structure of N-TPI/PEI blends were studied by using d.s.c. and SAXS. It has been found that the melt-quenched N-TPI/PEI blends exhibit miscibility over the entire composition range. The phase behaviour and crystallization behaviour of the melt-quenched blends on heat treatment vary considerably with temperature, heat treatment conditions, and composition.

EXPERIMENTAL

Materials

N-TPI with a weight-average molecular weight (M_w) of ca. 30 000 and PEI (ULTEM 1000, M_w ca. 30 000) were used as raw materials for the blends. Seven melt-quenched N-TPI/PEI blends (N-TPI/PEI = 100/0, 80/20, 60/40, 50/50, 40/60, 20/80, 0/100) were kindly supplied by Mitsui-Toatsu Chemicals, Inc. The blend samples were prepared by using a single screw extruder.

Sample preparation

The samples used for d.s.c. and SAXS measurements were prepared by heating the N-TPI/PEI blends on a pre-heated hot stage at temperatures of 260, 290, 300, 330, 340, 350, and 360°C for 2 h.

Differential scanning calorimetry

The d.s.c. thermograms were measured by using a Perkin-Elmer d.s.c.-7 calorimeter over the temperature range from room temperature to 400°C at a heating rate of 10°C min^{-1} in an atmosphere of nitrogen. The T_g was taken as the midpoint of the heat capacity increment. The heat of fusion of the blends was also measured during the heating scan. The degree of crystallinity of the N-TPI in the various blends was estimated from the melting endotherm on the basis of the value obtained for the heat of fusion of 100% crystalline N-TPI.

Small-angle X-ray scattering

The SAXS measurements were carried out with a 30 kV rotating-anode-type X-ray generator (Nihon-Denshi, JRX-30VA), equipped with a SAXS apparatus, using Ni-filtered CuKα radiation. The X-rays were collimated by a three-pinhole slit system. A one-dimensional, position-sensitive proportional counter was used to measure the SAXS intensity distribution. The distance between the sample and the detector was 540 mm. The raw SAXS intensity profiles were corrected for the background intensity, I_{back}, which represents the air scattering. The slope of Is^4 vs. s^4 ($s = 2\sin\theta/\lambda$) was used to obtain the diffraction intensity contribution from the thermal density fluctuation, I_f[4,20]. After the subtraction of I_f, the corrected intensity profile was used for quantitative analysis.

RESULTS AND DISCUSSION

Miscibility of the N-TPI/PEI blends in the amorphous state

The d.s.c. thermograms of the melt-quenched N-TPI/PEI blends on heating are given in *Figure 1*. As

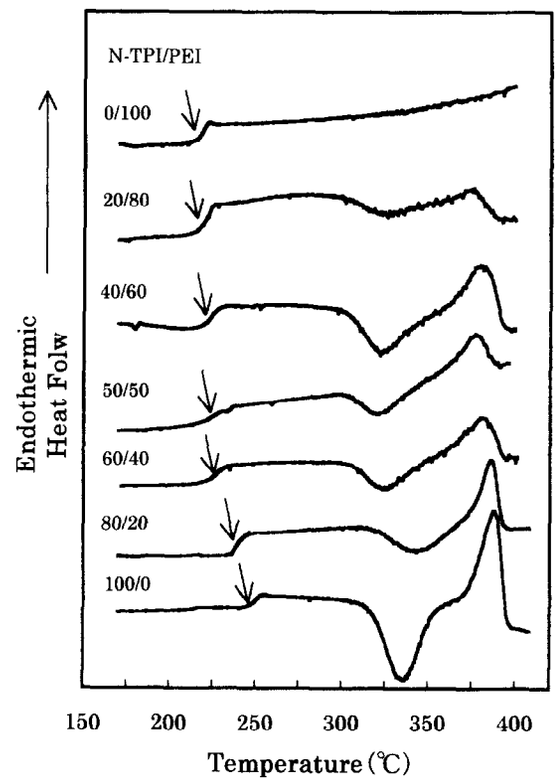

Figure 1 D.s.c. thermograms of the melt-quenched N-TPI/PEI blends with different compositions; arrows indicate the glass transition temperatures

illustrated, all of the blends exhibit a single glass transition over the entire composition range, thus indicating that N-TPI and PEI are fully miscible in the amorphous state. These results are in agreement with the observations of Crevecoeur and Groeninckx[2] and Hsiao and Sauer[6] on melt-quenched PAEK/PEI blends.

In general, the glass transition behaviour of the miscible blends can be analysed by using the Fox equation[21], as follows:

$$1/T_g = w_1/T_{g1} + w_2/T_{g2} \quad (1)$$

or the Gordon–Taylor equation[22]:

$$T_g \frac{w_1 T_{g1} + k w_2 T_{g2}}{(w_1 + k w_2)} \quad (2)$$

where w_1 and w_2 represent the weight fractions of the blend constituents and T_{g1} and T_{g2} their corresponding glass transition temperatures; k in equation (2) is an adjustable parameter.

In *Figure 2*, the glass transition temperatures (T_gs) of the amorphous N-TPI/PEI blends are plotted as a function of blend composition. The solid and dotted lines in *Figure 2* are predicted from the Fox and the Gordon–Taylor equations, respectively. As can be seen from this figure, the observed T_gs of the amorphous N-TPI/PEI blends fit the Gordon–Taylor equation (with a parameter k of 0.55), rather than the Fox equation.

As *Figure 1* shows, the N-TPI/PEI blends, with the exception of pure PEI, give a crystallization exotherm in each d.s.c. thermogram, indicating that N-TPI can crystallize from the miscible, amorphous state during heating in the calorimeter. The crystallization exotherm

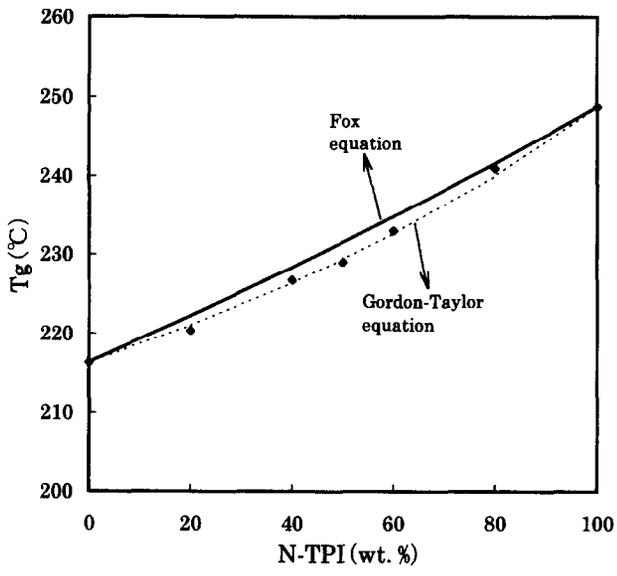

Figure 2 Glass transition temperature of the melt-quenched N-TPI/PEI blends *versus* N-TPI content. The symbol ◆ represents the experimental data; the solid line (—) and dotted line (···) are predicted from the Fox equation and the Gordon–Taylor equation (with a parameter k of 0.55) respectively

of the N-TPI/PEI blends, except for the N-TPI/PEI (80/20) system, is initiated at the lower temperature. It is conceivable that the crystallization of N-TPI in these blends is enhanced by the co-existing PEI in the initial stage of crystallization. This is quite different from the case of the PEEK/PEI blends. In these latter blends, the addition of PEI decreases the crystallization rate of the PEEK and makes the exotherm peak in the d.s.c. heating scan shift to a higher temperature with an increasing PEI component[6]. Another noticeable phenomenon is that the exotherms of the blends, in contrast to that of pure N-TPI, tail to the higher temperatures. This may be suggesting that the crystallization of N-TPI in these blends is hindered by the co-existing PEI segments in the later stage of crystallization.

The above observations suggest that the effect of blending of PEI on the crystallization behaviour of N-TPI is very complex and varies depending upon the blend composition. It seems that further information concerning the crystallization kinetics of N-TPI in the N-TPI/PEI blends is necessary before a thorough explanation can be achieved. Detailed studies of the isothermal crystallization kinetics of the blends are now in progress, and the results will be reported elsewhere.

Phase behaviour in N-TPI/PEI blends

In order to investigate the phase behaviour of the N-TPI/PEI blends, the melt-quenched amorphous samples were heat treated at 260, 290, 300, 330, 340, 350 and 360°C for 2 h on a pre-heated hot stage. The temperature of the blends was momentarily increased to a desired crystallization temperature (T_c). After cooling to room temperature, the samples were then subjected to the d.s.c. measurements. The blend sample which has been heat-treated at T °C will hereafter be abbreviated as the N-TPI/PEI blend (T).

The d.s.c. thermograms of the N-TPI/PEI blends (260) are shown in *Figure 3*. All of the blends, except for the pure PEI system, exhibit a crystallization exotherm in

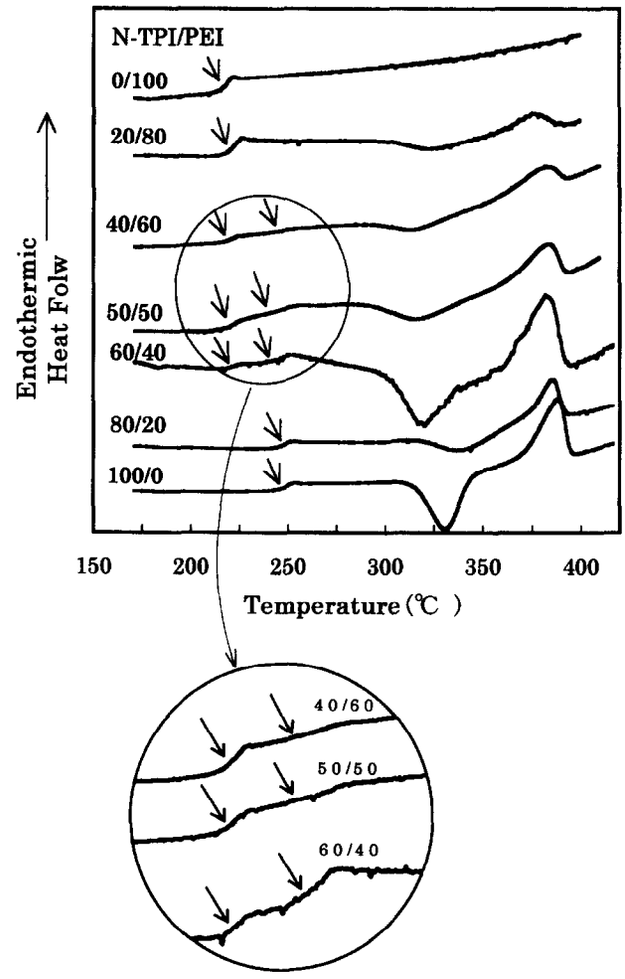

Figure 3 D.s.c. thermograms of N-TPI/PEI blends with different compositions which have been heat treated at 260°C for 2 h; melt-quenched blends were heat treated on a pre-heated hot plate, followed by cooling to room temperature. Enlarged details of the d.s.c. thermograms of certain blends (N-TPI/PEI = 60/40, 50/50, 40/60) are also shown

their d.s.c. thermograms, indicating that these blends still remain in the amorphous state even after heat treatment at 260°C. This seems to indicate that the mobility of the N-TPI segments is not enough for the crystallization of N-TPI to take place. The heat-treatment temperature (260°C) is higher than the T_g of N-TPI by only 5°C.

The N-TPI/PEI blends (260: N-TPI/PEI = 60/40, 50/50, 40/60) exhibit a pair of glass transitions, as can be clearly seen in the enlarged sections, while the N-TPI/PEI blends (260: N-TPI/PEI = 80/20, 20/80) exhibit a single glass transition. The T_gs of the N-TPI/PEI blend (260) are plotted against the N-TPI composition in *Figure 4*. As illustrated, the upper and lower T_g values of the N-TPI/PEI blends (260: N-TPI/PEI = 60/40, 50/50, 40/60) are nearly equal to those of the (260: N-TPI/PEI = 80/20) and (260: N-TPI/PEI = 20/80) blends. It seems likely that the N-TPI-rich phase and PEI-rich phase are separated from the miscible, amorphous phase during heat treatment at 260°C.

The N-TPI/PEI blends (290, 300, 330, 340) gave similar d.s.c. thermograms. As an example, only the d.s.c. thermograms of the N-TPI/PEI blends (330) are shown in *Figure 5*. A crystallization exotherm is no longer observed in these thermograms, indicating that the N-TPI components crystallize during the heat treatment at these temperatures.

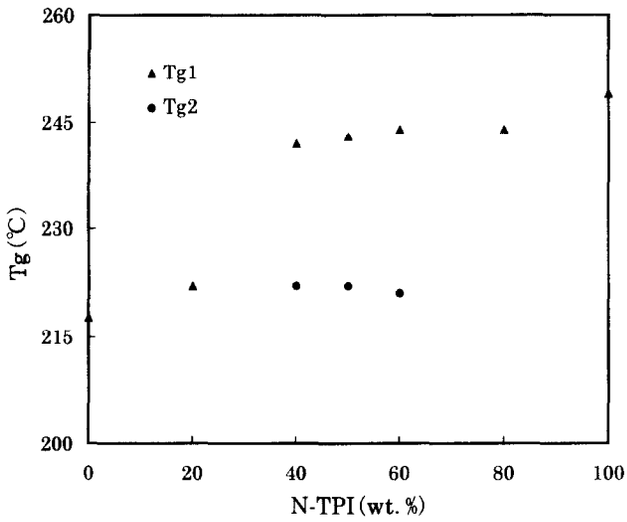

Figure 4 Glass transition temperature of N-TPI/PEI blends which have been heat treated at 260°C *versus* N-TPI content

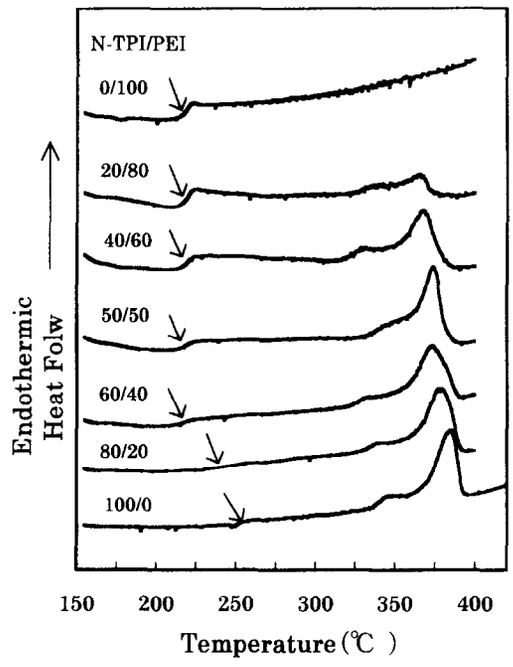

Figure 5 D.s.c. thermograms of N-TPI/PEI blends with different compositions which have been heat-treated at 330°C for 2 h; melt-quenched blends were heat treated on a pre-heated hot plate, followed by cooling to room temperature

The T_g values of N-TPI/PEI blends (290, 300, 330, 340) are plotted as a function of the weight fraction of N-TPI in *Figure 6*. Only the values of the N-TPI/PEI blend (290, 300, 330, 340: N-TPI/PEI = 80/20) can be approximately related to the Gordon–Taylor equation with $k = 0.55$, indicating that N-TPI is still miscible with PEI in the amorphous region. On the other hand, the N-TPI/PEI blends (290, 300, 330, 340: N-TPI/PEI = 60/40, 50/50, 40/60, 20/80) give a single T_g, similar to that of pure PEI (217°C). It seems reasonable to assume that PEI is phase-separated from the amorphous N-TPI region.

Based on the above observations, we could conclude that the N-TPI/PEI blends (290, 300, 330, 340: N-TPI/PEI = 80/20) consist of lamellar crystals of N-TPI and

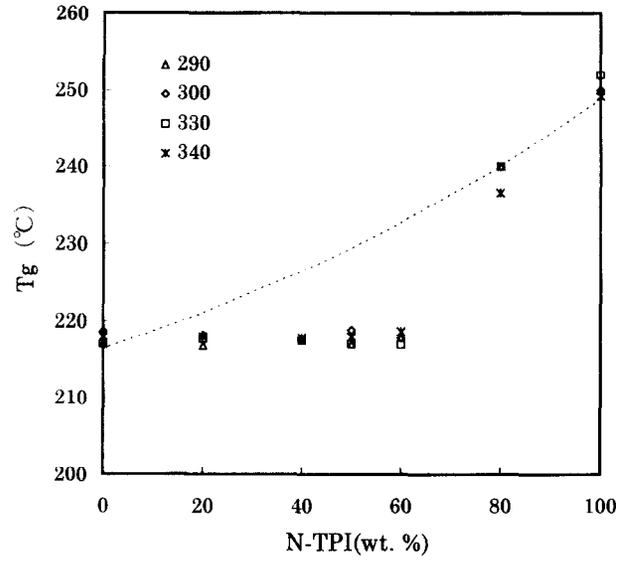

Figure 6 Glass transition temperatures of annealed N-TPI/PEI blends *versus* N-TPI content; melt-quenched blends were heat treated at 290, 300, 330, and 340°C for 2 h, followed by cooling to room temperature. The dotted line (···) is predicted from the Gordon–Taylor equation

the miscible N-TPI/PEI amorphous region, while the N-TPI/PEI blends (290, 300, 330, 340: N-TPI/PEI = 60/40, 50/50, 40/60, 20/80) consist of lamellar crystals of N-TPI, the N-TPI rich amorphous region, and the phase-separated PEI amorphous region. It should be noticed that no glass transition arising from the N-TPI rich amorphous region can be detected in their thermograms. It seems likely that the heat capacity increment below and above the T_g of the N-TPI rich region is too small to be detected by d.s.c. measurements. This observation can be explained by assuming that the mobility of the amorphous N-TPI segments are constrained by the lamellar crystals of N-TPI. On the other hand, N-TPI segments do not exist in the phase-separated PEI amorphous region, because the T_g values of the N-TPI/PEI blends (290, 300, 330, 340: N-TPI/PEI = 60/40, 50/50, 40/60, 20/80) are very similar to that of pure PEI. It can be suggested that the amorphous segments of N-TPI are constrained by the lamellar crystals and therefore they cannot diffuse to the PEI region. The above considerations lead us to the conclusion that in these N-TPI/PEI blends (60/40, 50/50, 40/60, 20/80), the phase separation takes place simultaneously with the crystallization of N-TPI during heat treatment at 290–330°C.

Hsiao and Sauer reported the glass-transition behaviour of PEEK/PEI blends in the amorphous and semicrystalline states[6]. According to their results, the T_g values of the PEEK/PEI blends vary with the blend composition both in the amorphous and semicrystalline states, although the values of the completely crystallized blends deviate from the Fox equation. The PEKK/PEI blends give similar results. These results indicate that PEEK and PEKK are miscible with PEI even in the semicrystalline state. This is evidently not the case in our system, because the phase separation occurs during the heat treatment of N-TPI/PEI blends at 260–330°C.

The d.s.c. thermograms of the N-TPI/PEI blends (360) exhibit a single glass transition and a crystallization exotherm is no longer observed. The N-TPI/PEI blends

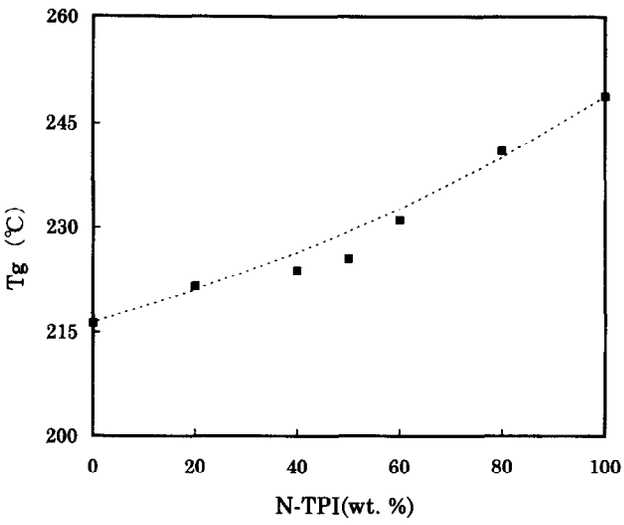

Figure 7 Glass transition temperatures of annealed N-TPI/PEI blends, heat treated at 360°C for 2 h, plotted against N-TPI content. The dotted line (···) is predicted from the Gordon–Taylor equation

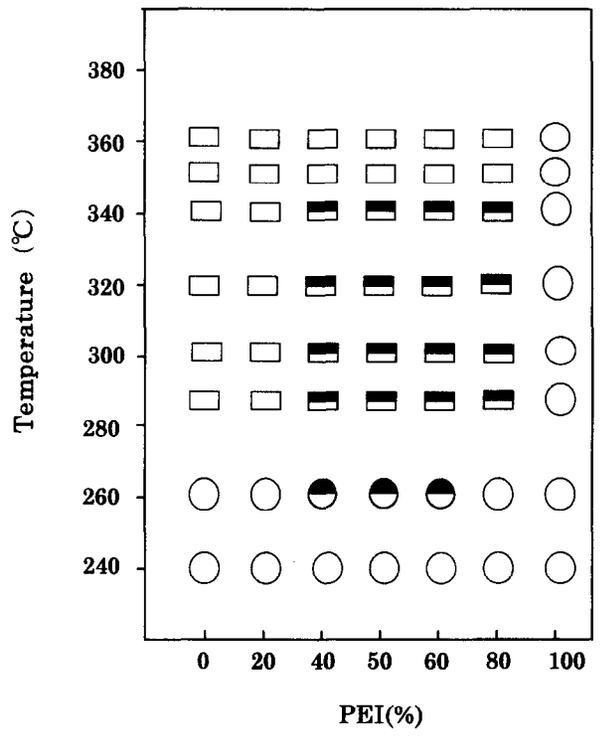

Figure 8 Phase diagram of the N-TPI/PEI blends: (○) misible amorphous state; (◓) phase-separated amorphous state; (□) semicrystalline state with miscible amorphous region (▣) semicrystalline state with phase-separated amorphous region

(350) gave similar results. The plot of the T_g values of N-TPI/PEI blends (360) *versus* the blend composition is illustrated in *Figure 7*. As illustrated, the values of these blends decrease with increasing PEI contents. Evidently, N-TPI is miscible with PEI in the amorphous region over the entire composition range, although crystallization of N-TPI takes place. It is interesting to note that the T_g behaviour of the N-TPI/PEI blends (360) is quite different from that of the N-TPI/PEI blends (290–340). It seems reasonable to assume that the higher heat-treatment temperature (>350°C) is favourable for maintaining the miscible state in the amorphous region. The thermal behaviour of the N-TPI/PEI blends (360) are similar to those of the heat-treated PAEKs/PEI blends[6].

The phase behaviour of the N-TPI/PEI blends which have been treated in the temperature range from 260 to 360°C are summarized in *Figure 8*. As shown, the following four states develop depending on the heat-treatment temperatures and the blend compositions:

1. A miscible amorphous state in the melt-quenched N-TPI/PEI blends.
2. A phase-separated amorphous state in the N-TPI/PEI blends which have been heat treated at 260°C.
3. A semicrystalline state with a phase-separated amorphous region in the N-TPI/PEI blends which have been heat-treated in the temperature range from 290 to 340°C.
4. A semicrystalline state with a miscible amorphous region in the N-TPI/PEI blends which have been heat treated at temperatures above 350°C.

It is possible to conclude from the results given above that N-TPI is miscible with PEI in the amorphous region at temperatures above 350°C, and that phase separation occurs simultaneously with the crystallization of N-TPI over the temperature range from 290 to 340°C.

Morphology of the N-TPI/PEI blends

In the previous section, it was confirmed from d.s.c. studies that phase separation between N-TPI and PEI occurs simultaneously with the crystallization of N-TPI when the melt-quenched N-TPI/PEI blends were heat treated over the temperature range from 290 to 340°C. On the other hand, phase separation did not occur during heat treatment at temperatures above 350°C. The influences of the phase separation and the crystallization on the semicrystalline morphology of N-TPI/PEI blends were studied by using small-angle X-ray scattering (SAXS).

Lorentz-corrected SAXS profiles of the N-TPI/PEI blend (330) with different compositions are shown in *Figure 9*. The long-spacing (L) of the stacked N-TPI crystals was estimated from the SAXS maximum (q_{max}) by using the relationship $L = 1/q_{max}$. It is evident that the long-spacing increases with increasing PEI content, suggesting that the PEI segments are located in the amorphous regions between the stacked N-TPI crystals. This result will be discussed later in this section by using a one-dimensional correlation function.

As illustrated in *Figure 9*, the maximum SAXS intensity (I_{max}) of the N-TPI/PEI blend (330: N-TPI/PEI = 80/20) is stronger than that of pure N-TPI which has been heat treated at the same temperature. On the other hand, the I_{max} decreases and the SAXS profile broadens as the PEI content increases above 40%. As is well known, the SAXS intensity is proportional to the square of the density difference between the crystalline and amorphous region ($\Delta\rho$), the regularity of the stacked lamellar structure, and the number of scattering entities. The densities of amorphous N-TPI and amorphous PEI are 1.323 and 1.279 g cm^{-3}, respectively. If the PEI segments are located between the N-TPI crystals, as previously described, the average $\Delta\rho$ between the N-TPI crystals and the amorphous layers becomes large. This could result in an increase in I_{max}. It seems reasonable to assume that the stacked lamellar structure is distorted,

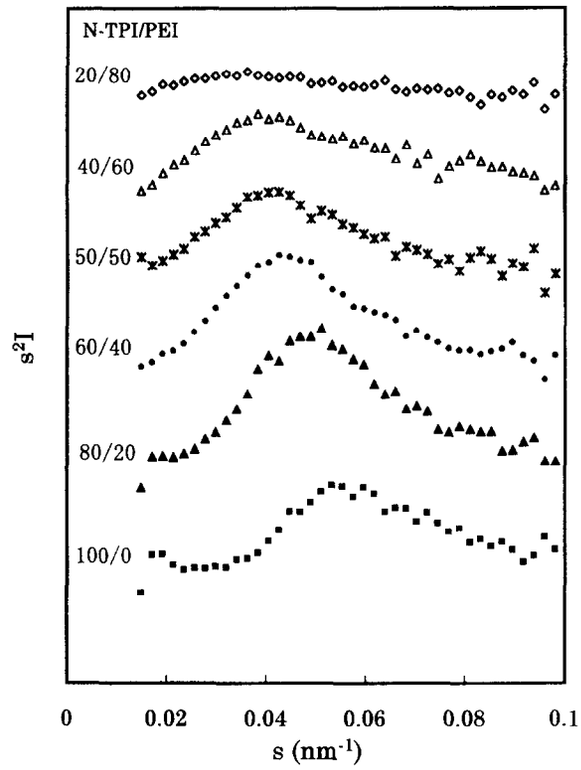

Figure 9 Lorentz-corrected SAXS patterns of N-TPI/PEI blends with different compositions which have been heat treated at 330°C

and the number of scattered entities decrease with increasing PEI, thus resulting in a decrease in I_{max} and a broadening of the SAXS profiles of the N-TPI/PEI blends (330: N-TPI/PEI = 60/40–20/80).

The electron-density correlation function is generally used to determine lamellar parameters such as the crystal and amorphous phase thicknesses. The correlation function, $K(z)$, can be evaluated from the scattering intensity, $I(s)$, by using the following equation:

$$K(z) = \int_0^\infty 4\pi s^2 I(s) \cos(2\pi sz)\, ds \qquad (3)$$

where s is the scattering vector ($s = 2\sin\theta/\lambda$) and z is the direction along which the electron-density distribution is measured. The obtained SAXS intensity was linearly extrapolated to $s = 0$. In addition, Porod's law[20], i.e. $I(s) \sim s^{-4}$, was used to extrapolate the intensity to $s = \infty$. A series of the corresponding correlation functions is shown in *Figure 10*.

The long-spacing, L_{max}, determined from the position of the first maximum of $K(z)$, is plotted against the N-TPI content in *Figure 11*, together with the L values determined from the Lorentz-corrected SAXS profiles. It is evident that both L_{max} and L tend to increase with increasing PEI content in a similar way. This result also supports the conclusion that the PEI segments are located between the N-TPI crystals. As is shown in *Figure 10*, the first maximum of the one-dimensional correlation function of the N-TPI/PEI blend (330) decreases appreciably with increasing PEI content, thus suggesting a distortion of the stacked lamellar structure.

The method of Strobl and Schneider is generally used to analyse the supermolecular structure of crystalline

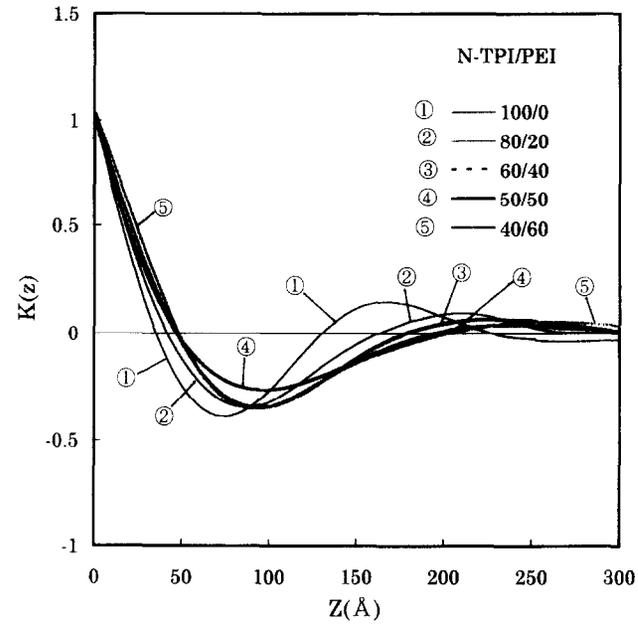

Figure 10 A series of correlation functions obtained using the scattering data from *Figure 9*

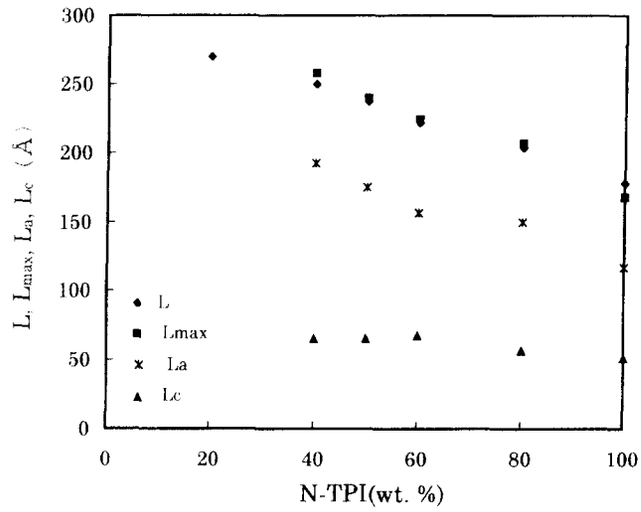

Figure 11 Lamellae parameters (L, L_{max}, L_c, L_a) *versus* N-TPI content: L, long-period estimated on the basis of Bragg's law; L_{max}, long-period determined from the one-dimensional correlation function, $\gamma(r)$; L_c, thickness of crystalline layer; L_a, thickness of amorphous layer

polymers[21]. Strictly speaking, this method is applicable to two-phase systems. Although the N-TPI/PEI blends (330) are composed of three phases (N-TPI crystals, an amorphous N-TPI region, and an amorphous PEI region), we have applied this method to determine the thickness of the crystals and the amorphous layer, because the difference between the density of the N-TPI crystals and the average density of the amorphous layer (N-TPI + PEI) is larger than that between the amorphous regions of N-TPI and PEI.

The stacked lamellar structure of N-TPI/PEI (330) was analysed by using the following equation:

$$x_1 x_2 L = B \qquad (4)$$

where x_1 and x_2 represent the linear fractions of phase 1 and 2, respectively, within the two-phase stacks

($x_1 + x_2 = 1$), and B is the first intercept with the $K(z) = 0$ line. It should be noted that one cannot determine from equation (4) which value of x_1 or x_2 represents the linear fraction of crystallinity. According to our studies on the semicrystalline structure of N-TPI with various molecular weights, the degree of crystallinity is of the order of 30%. In this present experiment (*Figure 10*) x_1 increases from 70 to 75% with increasing PEI content. Therefore, it seems reasonable to assign x_1 as the amorphous fraction, i.e. x_a. We use the values of L_{max} and x_1 to determine the thickness of the crystalline layer ($L_c = L_{max}x_2$) and the amorphous layer ($L_a = L_{max}x_1$). L_a and L_c are also plotted as a function of the N-TPI content in *Figure 11*. As can be seen in this figure, L_a increases linearly with increasing PEI content, while L_c is invariable with PEI content. These results also confirm the formation of the interlamellar morphology in the N-TPI/PEI blend (330).

The development of supermolecular structures in crystalline and amorphous polymer blends has been studied by several workers. Nishi and coworkers[22,23] and Nojima *et al.*[24–26], studied the blend system of poly(ϵ-caprolactone) (PCL) with polystyrene oligomer (PSO) on the basis of its phase diagram. It has been found that when PCL crystallizes, PSO can be accommodated in the amorphous layer of PCL to the limit of the miscibility. Further increases in the PSO component result in phase separation in the amorphous layer, with PSO finally being rejected outside of the PCL spherulites.

In the case of our N-TPI/PEI blends (290–340) (with compositions of N-TPI/PEI = 60/40, 50/50, 40/60), phase separation occurs simultaneously with crystallization of N-TPI, as indicated from the d.s.c. studies. The PEI segments are, nevertheless, still located between the lamellar crystals of N-TPI. The thickness of the amorphous layer, and consequently the long-spacing, continues to increase over the entire blend composition range. This phenomenon may be attributed to the low diffusivity between the amorphous N-TPI and PEI segments as a result of the rigidity of the N-TPI segments. *Figure 12* shows a schematic representation of the semicrystalline morphology of the N-TPI (a) and N-TPI/PEI blends, demonstrating that the PEI is miscible with the amorphous segments of N-TPI (b), or that the PEI is phase separated from the amorphous segments of N-TPI (c).

Structure (c) in *Figure 12* might not develop if phase separation occurs over the regions of 20 nm or above, because the long-spacing of the blends is of the order of 20 nm. It is reasonable to assume, therefore, that phase separation in the N-TPI/PEI blend (330) is confined to smaller regions, i.e. of the order of a few nm. The semicrystalline morphology of the N-TPI/PEI blend (330) is quite different from that of the PEEK/PEI blends, in which the PEI segments in the latter are extruded out from the amorphous layers between the stacked lamellar crystals of PEEK[3,6,7].

CONCLUSIONS

The phase behaviour and semicrystalline morphology of N-TPI/PEI blends were studied by using d.s.c. and SAXS. Melt-quenched amorphous blends with different compositions were used as raw materials. The SAXS data

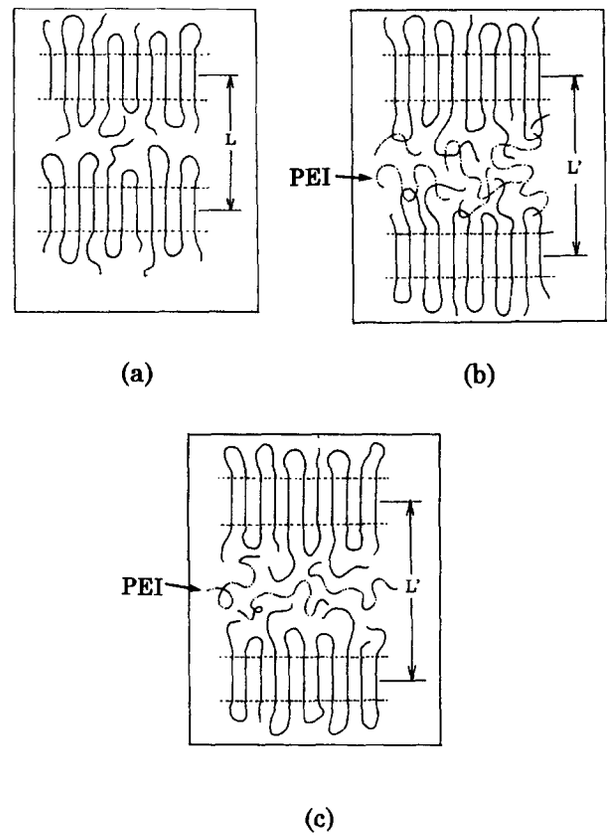

Figure 12 Schematic representation of the semicrystalline morphology of N-TPI (a) and the N-TPI/PEI blends, demonstrating that the PEI segments are miscible with the amorphous segments of N-TPI (b), or that they are phase-separated from the amorphous segments of N-TPI (c)

were analysed on the basis of the one-dimensional correlation function. The resulting results were obtained:

1. Melt-quenched amorphous N-TPI/PEI blends are miscible over the whole composition range.
2. Phase separation occurs when melt-quenched N-TPI/PEI blends are heat treated at 260°C; crystallization does not occur in this case.
3. Semicrystalline structures with phase-separated amorphous regions develop during heat treatment of the N-TPI/PEI blends at temperatures of 290–340°C.
4. Semicrystalline structures with miscible amorphous regions develop when the melt-quenched N-TPI/PEI blends are heat treated at temperatures above 350°C. Similar structures are also found in the melt-crystallized N-TPI/PEI blends.
5. PEI segments are incorporated in the amorphous layer between the N-TPI crystals, regardless of phase separation.

REFERENCES

1 Harris, J. E. and Robeson, J. M. *J. Appl. Polym. Sci.* 1988, **35**, 1877
2 Crevecoeur, G. and Groeninckx, G. *Macromolecules* 1991, **24**, 1190
3 Lee, C. H., Okada, T. and Inoue, T. *Kobunshi Ronbunshu* 1991, **48**, 581
4 Chen, H.-L. and Porter, R. S. *Polym. Eng. Sci.* 1992, **32**, 1870
5 Hudson, S. D., Davis, D. D. and Lovinger, A. J. *Macromolecules* 1992, **25**, 1759

6 Hsiao, B. S. and Sauer, B. B. *J. Polym. Sci. Polym. Phys. Edn* 1993, **31**, 901
7 Chen, H.-L. and Porter, R. S. *J. Polym. Sci. Polym. Phys. Edn* 1993, **31**, 1845
8 Harris, J. E. and Robeson, J. M. *J. Polym. Sci. Polym. Phys. Edn* 1987, **25**, 311
9 Karcha, R. J. and Porter, R. S. *J. Polym. Sci. Polym. Phys. Edn* 1993, **31**, 821
10 Okuyama, K., Salaitani, H. and Arikawa, H. *Macromolecules* 1992, **25**, 7261
11 Takahashi, T., Yuasa, S., Tsuji, M. and Sakurai, K. *J. Macromol. Sci. Phys.* 1994, **33**, 63
12 Ma, S. P., Sasaki, T., Sakurai, K. and Takahashi, T. *Polymer* 1994, **35**, 5619
13 Huo, P. P., Friler, J. B. and Cebe, P. *Polymer* 1993, **34**, 4387
14 Hsiao, B. S., Sauer, B. B. and Biswas, A. *J. Polym. Sci. Polym. Phys. Edn* 1994, **32**, 737
15 Ma, S. P., Yuasa, S., Tsuji, M., Sakurai, K. and Takahashi, T. *Kobunshi Robunshu* 1994, **51**, 329
16 Ma, S. P., Sasaki, T., Sakurai, K. and Takahashi, T. *Kobunshi Robunshu* 1995, **52**, 336
17 Furukawa, H., Morita, A. and Koba, T. *Polym. Prepr. Jpn* 1993, **42**, 3917
18 Tsutsumi, T., Morikawa, S., Nakakura, T., Shimamura, K., Takahashi, T., Koga, N., Ohta, M., Morita, A. and Yamaguchi, A. *Eur. Pat. Appl. 90312859.3* 1990
19 Sauer, B. B. and Hsiao, B. S. *Polymer* 1993, **34**, 3315
20 Porod, G. *Kolloid Z.* 1951, **124**, 83
21 Strobl, G. R. and Schneider, M. J. *J. Polym. Sci. Polym. Phys. Edn* 1980, **18**, 1343
22 Tanaka, H. and Nishi, T. *Phys. Rev. Lett.* 1985, **55**, 1102
23 Tanaka, H. and Nishi, T. *Phys. Rev. A* 1989, **39**, 783
24 Nojima, S., Terashima, T. and Ashida, T. *Polymer* 1989, **27**, 1007
25 Nojima, S., Satoh, K. and Ashida, T. *Macromolecules* 1991, **24**, 942
26 Nojima, S., Kato, K., Ono, M. and Ashida, T. *Macromolecules* 1992, **25**, 1922